JOURNAL OF CHEMICAL & ENGINEERING DATA

ARTICLE

pubs.acs.org/jced

Equilibrium Phase Behavior of Aqueous Two-Phase Systems Containing 1-Alkyl-3-methylimidazolium Tetrafluoroborate and Ammonium Tartrate at Different Temperatures: Experimental Determination and Correlation

Juan Han, Yun Wang, Yanfang Li, Cuilan Yu, and Yongsheng Yan*

School of Chemistry and Chemical Engineering, Jiangsu University, 301 Xuefu Road, Zhenjiang 212013, China

ABSTRACT: Binodal data of the aqueous 1-alkyl-3-methylimidazolium tetrafluoroborate ([$C_n$mim]BF_4, n = 2, 3, 4) + ammonium tartrate ($(NH_4)_2C_4H_4O_6$) aqueous two-phase systems (ATPSs) have been determined experimentally at T = (288.15, 298.15 and 308.15) K. Three empirical equations were used to correlate the binodal data. The effect of temperature on the binodal curves was also studied, and it was observed that the biphasic region expanded with a decrease in temperature. The calculated effective excluded volume (EEV) and the binodal curves plotted in molality both indicate that the phase-separation abilities of the investigated ILs are in the order of [C_4mim]BF_4 > [C_3mim]BF_4 > [C_2mim]BF_4. On the basis of the empirical equation of binodal curve with the highest accuracy and lever rule, the liquid−liquid equilibrium data were calculated by MATLAB. The reliability of the tie-line compositions was proved by the empirical correlation equations given by Othmer−Tobias and Bancroft equations. Furthermore, a relatively simply two-parameter equation was successfully used to correlate the tie-line data. Finally, the slope of the tie lines decreases with an increase in temperature and increases with an increase in cation alkyl chain length of the investigated ILs.

INTRODUCTION

Aqueous two-phase systems (ATPSs), which have often been a favored choice in liquid−liquid extraction, are well-known as green separation systems and are able to replace conventional organic compounds. Typical ATPSs are generated by mixing two different polymers or one polymer and one salt at certain contain concentrations in an aqueous solution.[1−3] Liquid−liquid extraction utilizing these ATPSs has been used to separate and purify biological products from the complex mixtures in which they are produced.[2,3]

Ionic liquids (ILs) are the latest molecular class that has attracted attention for green chemistry applications owing to their unique properties such as negligible volatility, nonflammability, excellent solvent power for organic and inorganic compounds, and relative ease of structure modification to elicit the desired physical properties.[4] ILs and ATPSs have been combined together for the first time by Rogers and his co-workers in 2003.[5] These new ATPSs have many advantages shared by ILs and ATPSs, such as low viscosity, little emulsion formation, no need of using volatile organic solvent, quick phase separation, high extraction efficiency, and gentle biocompatible environment, and have been successfully used to separate drugs,[6,7] proteins,[8,9] amino acids,[10,11] and antibiotics.[12,13]

To aid the design and process optimization of IL-based aqueous two-phase extraction technique, detailed information on the phase diagrams, liquid−liquid equilibrium (LLE) data and the physicochemical properites of these systems is desirable. At the present time, liquid−liquid equilibria of IL−salt ATPSs,[14−20] IL−carbohydrate ATPSs,[21−26] and IL−amino acid ATPSs[27] have been widely reported. In these studies, due to inorganic salts have the stronger capibility of salting-out of IL, IL−inorganic salt ATPSs are now in widespread use. However, high concentrations of these inorganic salts are not desirable in the effluent streams due to environmental problems. Recently, Zafarani-Moattar and his co-workers have used citrate salt as a substitute for inorganic salt in [C_4mim]X−salt (X = Cl and Br) ATPSs[28−30] due to its biodegradability and nontoxicity. In our previous research, we have reported the phase diagrames and LLE data of [C_4mim]BF_4−$Na_3C_6H_5O_7$/$(NH_4)_3C_6H_5O_7$/$Na_2C_4H_4O_6$/$NaC_2H_3O_2$ ATPSs.[31,32] In continuation of our previous work on the phase equilibrium properties of IL−inorganic salt ATPSs, here we report the phase diagrams and the compositions of phases for the 1-alkyl-3-methylimidazolium tetrafluoroborate ([$C_n$mim]BF_4, n = 2, 3, 4)−ammonium tartrate ($(NH_4)_2C_4H_4O_6$) ATPSs at T = (288.15, 298.15, and 308.15) K that have not been published previously. The obtained results are necessary for the design and optimization of extraction processes, understanding the general factors determining the partition of solutes and particles in such ATPSs, and the development and testing of both thermodynamic and mass transfer models of ATPSs.

In this work, the phase diagrams for the systems containing ILs ([C_2mim]BF_4, [C_3mim]BF_4, [C_4mim]BF_4) and $(NH_4)_2C_4H_4O_6$ have been determined experimentally. Suitable equations were used to correlate the binodal curve and the tie-line data for the investigated systems. These data provide a possible basis for the prediction of phase composition when such data are not available. In addition, the effect of temperature and the type of IL on binodal curves and tie lines of the investigated systems were dicussed. The effective excluded volume (EEV) values obtained from the binodal model for these ATPSs and the phase-separation abilities of the investigated ILs were also discussed.

Received: June 20, 2011
Accepted: August 3, 2011
Published: August 23, 2011

Table 1. Binodal Data for the $[C_2mim]BF_4$ (1) + $(NH_4)_2$-$C_4H_4O_6$(2) + H_2O (3) ATPSs at T = (288.15, 298.15, and 308.15) K and Pressure p = 0.1 MPa[a]

T = 288.15 K		T = 298.15 K		T = 308.15 K	
100 w_1	100 w_2	100 w_1	100 w_2	100 w_1	100 w_2
81.50	0.23	80.29	0.28	74.54	0.98
75.87	0.62	76.77	0.54	71.98	1.40
72.01	0.95	73.53	1.06	68.62	1.92
69.41	1.34	70.56	1.49	66.15	2.49
67.61	1.59	67.47	1.89	64.32	2.79
64.14	2.07	65.82	2.04	60.95	3.56
63.28	2.29	62.61	2.71	60.83	3.57
59.71	3.11	61.82	2.99	57.54	4.28
57.24	3.62	58.19	3.70	56.77	4.53
55.12	4.12	56.66	4.12	50.99	5.99
52.58	4.77	55.34	4.32	51.01	5.94
50.50	5.31	53.69	4.73	47.16	7.13
48.94	5.77	51.93	5.27	46.27	7.58
46.43	6.32	49.77	5.78	44.54	8.17
44.00	7.30	47.44	6.49	42.85	8.72
42.24	7.89	46.63	6.77	42.69	8.77
40.55	8.42	43.37	7.77	40.56	9.65
39.89	8.69	41.48	8.45	39.11	10.08
37.63	9.37	40.29	8.82	39.05	10.08
36.01	9.85	38.44	9.50	37.38	10.75
34.45	10.68	35.95	10.43	35.54	11.51
33.12	11.01	33.72	11.26	34.70	11.88
31.17	11.79	31.60	12.07	32.85	12.56
28.88	12.80	29.43	12.99	31.62	13.15
27.33	13.35	28.65	13.40	30.85	13.43
25.97	13.87	27.04	14.03	28.66	14.25
23.93	14.79	25.30	15.06	26.78	15.42
22.79	15.58	24.75	15.22	26.70	15.44
21.60	16.36	22.47	16.54	24.96	16.43
20.52	16.72	19.52	18.68	23.78	17.11
19.86	17.37	17.66	20.32	22.19	18.17
18.89	17.98	16.57	21.20	20.80	19.07
17.49	19.05			19.04	20.44
16.56	19.52				

[a] Standard uncertainties u are $u(w)$ = 0.001, $u(T)$ = 0.05 K, and $u(p)$ = 10 kPa.

Table 2. Binodal Data for the $[C_3mim]BF_4$ (1) + $(NH_4)_2$-$C_4H_4O_6$(2) + H_2O (3) ATPSs at T = (288.15, 298.15, and 308.15) K and Pressure p = 0.1 MPa[a]

T = 288.15 K		T = 298.15 K		T = 308.15 K	
100 w_1	100 w_2	100 w_1	100 w_2	100 w_1	100 w_2
71.89	2.23	77.32	2.37	73.73	3.33
68.62	2.51	73.24	2.73	70.08	3.92
63.82	2.99	71.74	2.92	67.67	4.16
61.00	3.32	67.33	3.66	66.15	4.45
58.08	3.58	63.39	4.08	62.58	4.95
55.75	3.82	61.15	4.52	59.73	5.38
53.71	4.01	59.94	4.6	58.61	5.59
51.26	4.38	57.60	5.12	55.67	6.11
48.85	4.66	55.25	5.42	54.67	6.28
47.05	4.91	52.69	5.85	52.02	6.74
45.15	5.21	50.35	6.18	50.39	7.02
43.50	5.42	47.11	6.69	48.72	7.38
41.75	5.79	44.63	7.20	46.95	7.72
40.01	6.04	42.39	7.63	44.25	8.26
37.38	6.61	39.97	8.11	42.16	8.80
35.50	7.00	38.01	8.60	41.18	9.07
33.41	7.61	36.54	8.90	39.56	9.35
32.18	7.92	33.60	9.79	38.66	9.63
30.87	8.31	32.35	10.09	36.40	10.36
29.51	8.79	30.58	10.70	35.32	10.53
28.29	9.21	28.99	11.25	34.36	10.88
26.94	9.78	26.67	12.08	33.40	11.17
25.95	10.14	25.77	12.40	32.65	11.39
24.75	10.68	24.20	13.21	31.60	11.65
23.62	11.25	23.55	13.58	30.02	12.14
22.71	11.71	22.19	14.28	28.09	12.98
22.15	12.08	21.76	14.47	26.92	13.28
20.85	12.94	20.77	15.09	25.29	14.06
19.88	13.60	19.51	16.02	23.52	15.03
18.98	14.26	18.28	16.99	22.11	15.74
17.91	15.09	16.97	18.06	20.17	17.06
17.02	15.81	15.12	19.80	18.03	18.68
15.69	17.08				
14.09	18.73				

[a] Standard uncertainties u are $u(w)$ = 0.001, $u(T)$ = 0.05 K, and $u(p)$ = 10 kPa.

EXPERIMENTAL SECTION

Materials. $[C_2mim]BF_4$, $[C_3mim]BF_4$, and $[C_4mim]BF_4$ were purchased from Chenjie Chemical Co., Ltd. (Shanghai, China) with a quoted purity of greater than 0.99 mass fraction and was used without further purification. $(NH_4)_2C_4H_4O_6$ were analytical grade reagents (GR, min. 99% by mass fraction), which were obtained from Sinopharm Chemical Reagent Co., Ltd. (Shanghai, China). All other reagents were of analytical grade, and double distilled deionized water was used in the experiments.

Apparatus and Procedure. The binodal curves were determined by the titration method (cloud point method). A glass vessel, volume 50 cm^3, was used to carry out the phase equilibrium determinations. The glass vessel was provided with an external jacket in which water at constant temperature was circulated using a DC-2008 water thermostat (Shanghai Hengping Instrument Factory, China). The temperature was controlled to within ±0.05 K. An IL solution of known mass fraction was taken into the vessel, and then a salt solution of known mass fraction was added dropwise to the vessel until the mixture became turbid or cloudy. The composition of this mixture was noted. Afterward, water was added dropwise to the vessel to get a clear one-phase system, and the procedure was repeated and so on. The composition of the mixture for each point on the binodal curve was calculated by mass using an analytical balance (Model BS 124S, Beijing Sartorius Instrument Co., China) with a precision of $\pm 1.0 \times 10^{-7}$ kg. The maximum uncertainty was found to be 0.001 in determining the mass fraction of both IL and salt by titration method used.

Table 3. Binodal Data for the $[C_4mim]BF_4$ (1) + $(NH_4)_2C_4H_4O_6$(2) + H_2O (3) ATPSs at T = (288.15, 298.15, and 308.15) K and Pressure p = 0.1 MPa[a]

T = 288.15 K		T = 298.15 K		T = 308.15 K	
100 w_1	100 w_2	100 w_1	100 w_2	100 w_1	100 w_2
75.88	0.35	74.78	0.53	73.71	0.80
70.19	0.45	71.33	0.63	69.93	1.01
66.27	0.62	63.79	0.98	64.18	1.36
62.33	0.74	60.71	1.16	61.46	1.60
57.24	0.92	55.90	1.41	59.28	1.79
53.59	1.00	53.05	1.59	57.18	1.95
50.79	1.10	50.31	1.75	54.43	2.21
47.31	1.31	47.96	2.02	52.08	2.48
45.01	1.40	46.08	2.17	49.87	2.64
42.57	1.54	44.34	2.34	47.89	2.89
39.46	1.71	42.90	2.50	44.70	3.26
37.81	1.81	39.71	2.80	42.59	3.51
35.45	1.92	38.38	2.93	39.61	3.89
33.23	2.14	37.07	3.06	37.19	4.22
31.46	2.32	34.46	3.33	35.89	4.48
30.23	2.45	32.33	3.60	33.54	4.92
27.55	2.92	30.29	3.90	31.06	5.26
26.33	3.21	28.89	4.24	30.16	5.45
24.14	3.69	27.87	4.49	27.01	6.18
22.86	4.03	26.34	4.87	25.97	6.46
21.37	4.65	26.25	4.92	24.91	6.76
19.75	5.38	24.83	5.39	22.89	7.48
18.85	5.92	23.63	5.74	21.01	8.34
18.17	6.30	22.38	6.21	19.91	8.93
17.06	6.97	20.99	6.92	18.90	9.48
16.08	7.73	18.85	7.87	18.02	9.92
15.24	8.57	17.87	8.37	17.19	10.40
14.30	9.28	16.74	9.25	16.30	11.06
13.70	10.10	14.83	10.78	15.28	11.98
12.37	11.67	13.71	11.90	14.39	12.79
11.10	13.05	12.68	13.02	13.25	14.03
10.44	14.60	11.36	14.77	12.29	15.10
		10.27	16.59	11.15	16.55

[a] Standard uncertainties u are $u(w)$ = 0.001, $u(T)$ = 0.05 K, and $u(p)$ = 10 kPa.

The tie lines (TLs) were determined by a gravimetric method described by Merchuk et al.[33] For the TL determinations a mixture at the biphasic region was prepared by mixing an appropritate mass of IL (m_1), $(NH_4)_2C_4H_4O_6$ (m_2), and water (m_3), vigorously stirred and allowed to reach equilibrium by the separation of both phases for 12 h at T = (288.15, 298.15, and 308.15) K using small ampules especially designed for the purpose. After the separation step, both top phase (m_t) and bottom phase (m_b) were weighted, respectively. Each individual TL was determined by application of the lever rule to the relationship between the top mass phase composition and the overall system composition.[33]

RESULTS AND DISCUSSION

Binodal Data and Correlation. The binodal data, for the $[C_2mim]BF_4$/$[C_3mim]BF_4$/$[C_4mim]BF_4$ + $(NH_4)_2C_4H_4O_6$ + water ATPSs, representing the minimum concentration required for the formation of two phases at temperatures (288.15, 298.15, and 308.15) K are given in Tables 1, 2, and 3. The binodal data were correlated by the following equations

Table 4. Values of Parameters of eq 1 for the $[C_2mim]BF_4$/$[C_3mim]BF_4$/$[C_4mim]BF_4$ (1) + $(NH_4)_2C_4H_4O_6$(2) + H_2O (3) ATPSs at T = (288.15, 298.15, and 308.15) K

T/K	a	b	c	R^2	100 sd[a]
		$[C_2mim]BF_4 + (NH_4)_2C_4H_4O_6 + H_2O$			
288.15	0.94772	−2.73399	86.17716	0.99771	0.86
298.15	0.96241	−2.71021	72.67190	0.99439	1.32
308.15	1.00883	−2.76093	60.69227	0.99726	0.80
		$[C_3mim]BF_4 + (NH_4)_2C_4H_4O_6 + H_2O$			
288.15	1.85689	−6.22125	−19.22891	0.99913	0.47
298.15	1.70830	−4.95979	49.08778	0.99478	1.28
308.15	1.84762	−4.87623	48.99773	0.99774	0.71
		$[C_4mim]BF_4 + (NH_4)_2C_4H_4O_6 + H_2O$			
288.15	1.25341	−8.56481	−328.44018	0.98934	1.85
298.15	1.26812	−7.02211	−90.22630	0.99769	0.82
308.15	1.33869	−6.23934	7.94572	0.99599	1.12

[a] sd = $(\sum_{i=1}^{n}(w_1^{cal} - w_1^{exp})^2/n)^{0.5}$, where w_1^{exp} is the experimental mass fraction of IL in Tables 1−3 and w_1^{cal} is the corresponding data calculated using eq 1. n represents the number of binodal data.

$$w_1 = a \exp(bw_2^{0.5} - cw_2^3) \quad (1)$$

$$w_1 = a \times \ln(w_2 + c) + b \quad (2)$$

$$w_1 = \exp(a + bw_2^{0.5} + cw_2 + dw_2^2) \quad (3)$$

where w_2 is the mass fraction of salts, w_1 is the mass fraction of ILs, and a, b, c, and d are fitting parameters. These three equations have been widely used for the correlation of binodal data of IL-based ATPSs,[15,16,34] polymer-based ATPSs,[35,36] and hydrophilic alcohol-based ATPSs.[37,38] The fitting parameters obtained from the correlation of experimental binodal data along with the correlation coefficients (R^2) and the corresponding standard deviations (sd) of eqs 1 and 2 as well as eq 3 are given in Tables 4, 5, and 6, respectively. On the basis of the obtained R^2 and sd, it can be concluded that eq 3 shows more satisfactory accuracy in binodal data fitting for the investigated systems.

Eeffect of Temperature on Binodal Curves. Figure 1 shows the binodal boundavies obtained from turbidimeteric titrations at different temperatures. The region below the curves shown at each temperature in Figure 1 refers to homgeneous solutions and the region above to the two-phase region. The locus for the experimental binodals demonstrates an increase in the temperature caused an expansion of one-phase area. In other words, if one takes a sample on the binodal with a known composition, this mixture becomes a two-phase system by decreasing the temperature as we observed experimentally. A possible reason is that the effect of a decrease in temperature on the structure of water is qualitatively similar to that of a kosmotropic (structure-making) ion and therefore can promote the phase-forming ability in the investigated systems, as a favorable factor for the exclusion of the IL. More recently, the effect of temperature on the phase-forming ability in the $[C_4mim]BF_4$−Na_2CO_3/NaH_2PO_4 ATPSs,[20] $[C_4mim]Cl$−$K_3C_6H_5O_7$ ATPS,[28] and $[C_4mim]BF_4$-sucrose/maltose ATPSs[25]

Table 5. Values of Parameters of eq 2 for the $[C_2mim]BF_4$/$[C_3mim]BF_4$/$[C_4mim]BF_4$ (1) + $(NH_4)_2C_4H_4O_6$(2) + H_2O (3) ATPSs at T = (288.15, 298.15, and 308.15) K

T/K	a	b	c	R^2	100 sd[a]
		$[C_2mim]BF_4 + (NH_4)_2C_4H_4O_6 + H_2O$			
288.15	−0.36469	−0.36129	0.04060	0.99812	0.78
298.15	−0.35622	−0.3343	0.03931	0.99929	0.47
308.15	−0.40008	−0.35732	0.05387	0.99968	0.27
		$[C_3mim]BF_4 + (NH_4)_2C_4H_4O_6 + H_2O$			
288.15	−0.22854	−0.27883	−0.01078	0.99481	1.13
298.15	−0.33407	−0.41564	0.00359	0.99443	1.33
308.15	−0.35798	−0.43722	0.00264	0.99762	0.73
		$[C_4mim]BF_4 + (NH_4)_2C_4H_4O_6 + H_2O$			
288.15	−0.15348	−0.24098	−0.00231	0.97271	2.96
298.15	−0.18195	−0.26900	−0.00199	0.98560	2.04
308.15	−0.22213	−0.32632	−0.00052	0.99071	1.71

[a] sd = $(\sum_{i=1}^{n}(w_1^{cal} - w_1^{exp})^2/n)^{0.5}$, where w_1^{exp} is the experimental mass fraction of IL in Tables 1−3 and w_1^{cal} is the corresponding data calculated using eq 2. n represents the number of binodal data.

Table 6. Values of Parameters of eq 3 for the $[C_2mim]BF_4$/$[C_3mim]BF_4$/$[C_4mim]BF_4$ (1) + $(NH_4)_2C_4H_4O_6$(2) + H_2O (3) ATPSs at T = (288.15, 298.15, and 308.15) K

T/K	a	b	c	d	R^2	100 sd[a]
			$[C_2mim]BF_4 + (NH_4)_2C_4H_4O_6 + H_2O$			
288.15	−0.10455	−2.12465	−0.86755	−16.08806	0.99965	0.33
298.15	−0.14782	−1.17854	−4.28131	−5.10223	0.99961	0.34
308.15	−0.14329	−1.12575	−3.77574	−6.03449	0.99975	0.24
			$[C_3mim]BF_4 + (NH_4)_2C_4H_4O_6 + H_2O$			
288.15	0.34930	−3.19076	−9.19531	24.01053	0.99944	0.37
298.15	−0.36789	4.41274	−25.41841	40.09826	0.99958	0.36
308.15	−0.26147	3.33186	−20.41013	26.11338	0.99982	0.20
			$[C_4mim]BF_4 + (NH_4)_2C_4H_4O_6 + H_2O$			
288.15	0.40089	−11.60756	11.33918	10.38636	0.99435	1.33
298.15	0.13331	−5.15081	−8.42804	43.21816	0.99828	0.69
308.15	−0.06977	−0.96325	−19.28332	55.93209	0.9995	0.39

[a] sd = $(\sum_{i=1}^{n}(w_1^{cal} - w_1^{exp})^2/n)^{0.5}$, where w_1^{exp} is the experimental mass fraction of IL in Tables 1−3 and w_1^{cal} is the corresponding data calculated using eq 3. n represents the number of binodal data.

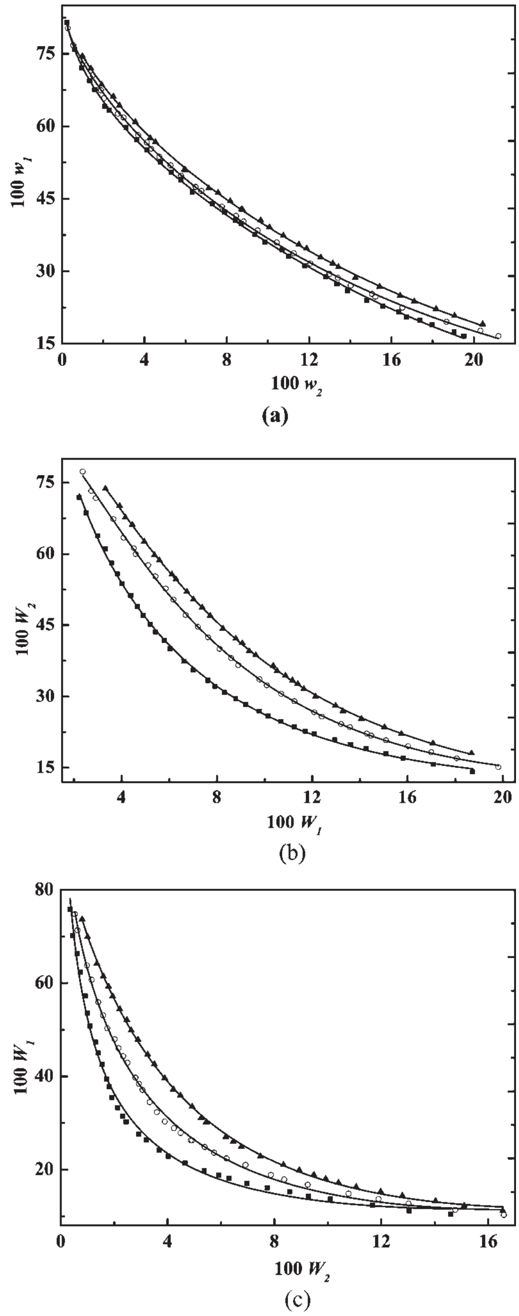

Figure 1. Effect of temperature on binodal curves of the $[C_2mim]BF_4$/$[C_3mim]BF_4$/$[C_4mim]BF_4$ (1) + $(NH_4)_2C_4H_4O_6$(2) + H_2O (3) ATPSs: (a) $[C_2mim]BF_4$; (b) $[C_3mim]BF_4$; (c) $[C_4mim]BF_4$; ■, 288.15 K; ○, 298.15 K; ▲, 308.15 K.

has also demonstrated that the two-phase area is expanded with a decrease in temperature. Actually, what appears to happen is that the interaction of the hydrophilic IL with surrounding water molecules, which is weakened in the presence of a kosmotropic salt (with the relatively strong affinity for water), is further diminished due to a decrease in temperature. Decreasing the temperature may be effective as a factor to enhance the formation of the water structure, and therefore the ability of the system for the mutually liquid−liquid demixing increases with decreasing temperature.

Effective Excluded Volume and Phase-Separation Abilities of ILs. The binodal model based on the statistical geometry methods is developed by Guan et al.[39] for aqueous polymer−polymer systems. In a previous work, our team extended the application of this model in the hydrophilic alcohol−salt ATPSs,[38,40] IL−salt ATPSs,[31,32] and poly(propylene glycol) (PPG)−salt ATPSs.[41,42] In this paper, the binodal equation for the $[C_2mim]BF_4$/$[C_3mim]BF_4$/$[C_4mim]BF_4$−$(NH_4)_2C_4H_4O_6$ ATPSs can be written as

$$\ln\left(V_{213}^{*}\frac{w_2}{M_2} + f_{213}\right) + V_{213}^{*}\frac{w_1}{M_1} = 0 \tag{4}$$

$$\ln\left(V_{213}^{*}\frac{w_2}{M_2}\right) + V_{213}^{*}\frac{w_1}{M_1} = 0 \tag{5}$$

Table 7. Values of Parameters of EEV of ILs Using eq 4 or 5 for the $[C_2mim]BF_4$/$[C_3mim]BF_4$/$[C_4mim]BF_4$ (1) + $(NH_4)_2C_4H_4O_6$(2) + H_2O (3) ATPSs at T = (288.15, 298.15, and 308.15) K

IL	T/K	$10^3V^*_{213}/(g\cdot mol^{-1})$	f_{213}	R^2	100 sd[a]
$[C_2mim]BF_4$	288.15	0.50455	0.13019	0.99794	0.83
	298.15	0.48778	0.13741	0.99843	0.71
	308.15	0.45467	0.15863	0.99946	0.36
$[C_3mim]BF_4$	288.15	0.73016		0.98750	1.86
	298.15	0.65241		0.99376	1.45
	308.15	0.61564		0.99768	0.75
$[C_4mim]BF_4$	288.15	1.17999		0.95400	3.98
	298.15	1.03734		0.97263	2.84
	308.15	0.92629		0.98308	2.33

[a] sd = $(\sum_{i=1}^{n}(w_1^{cal} - w_1^{exp})^2/n)^{0.5}$, where w_1^{exp} is the experimental mass fraction of IL in Tables 1−3 and w_1^{cal} is the corresponding data calculated using eq 4 or 5. n represents the number of binodal data.

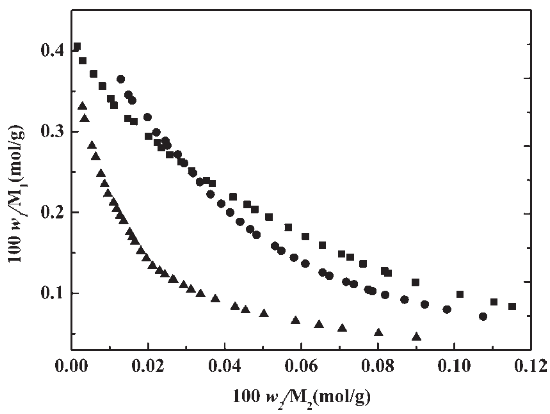

Figure 2. Effect of type of IL on the binodal curves plotted in molality for the $[C_2mim]BF_4$/$[C_3mim]BF_4$/$[C_4mim]BF_4$ (1) + $(NH_4)_2C_4H_4O_6$(2) + H_2O (3) ATPSs at ATPSs at 298.15 K: ■, $[C_2mim]BF_4$; ●, $[C_3mim]BF_4$; ▲, $[C_4mim]BF_4$.

where V^*_{213}, f_{213}, M_1, and M_2 are the scaled EEV of salt, the volume fraction of unfilled effective available volume after tight packing of salt molecules into the network of ionic liquid molecules in ionic liquid aqueous solutions, which includes the influence of the size of the water molecules, and molecular mass of ionic liquid and salt, respectively.

In the original application, eq 5 was used to correlate binodal data of polymer−polymer systems because of the marked difference in size between the two components. The f_{213} value will be very small and consequently can be neglected. The EEV represents the smallest spacing of an individual ionic liquid which will accepted an individual salt, so it reflects the compatibility of components in the same system. For the investigated systems, the EEV and f_{213} values obtained from the correlation of the experimental binodal along with the corresponding correlation coefficients (R^2) and standard deviations (sd) are given in Table 7. From the table, it was found that the parameter f_{213} was not so small as to be neglected for the $[C_2mim]BF_4$−$(NH_4)_2C_4H_4O_6$ ATPS, and eq 4 showed a much higher accuracy in bimodal data fitting than eq 5. Nevertheless, as for the $[C_3mim]BF_4$/$[C_4mim]BF_4$−$(NH_4)_2C_4H_4O_6$ ATPSs, there was no significant difference between these two equations in binodal data fitting, so a simplified eq 5 can be used. The scaled EEV of a same salt varies in different ILs because of the difference in size, shape, and interaction of molecules. From the Table 7, the rank order of the scaled EEV of $(NH_4)_2C_4H_4O_6$ in IL−water solvent is $[C_4mim]BF_4$ > $[C_3mim]BF_4$ > $[C_2mim]BF_4$ at the same temperature, which indicates that IL of shorter cation alkyl chain is easier to be excluded from the salt-rich phase to the IL-rich phase. To examine more closely the relation between the EEV values and phase-separation abilities of ILs, the binodals of the investigated systems are plotted in Figure 2, where

Table 8. Tie-Line Data for the $[C_2mim]BF_4$/$[C_3mim]BF_4$/$[C_4mim]BF_4$ (1) + $(NH_4)_2C_4H_4O_6$(2) + H_2O (3) ATPSs at T = (288.15, 298.15, and 308.15) K and Pressure p = 0.1 MPa[a]

	total system		IL-rich phase		salt-rich phase		slope	av
T/K	$100w_1$	$100w_2$	$100w_1^t$	$100w_2^t$	$100w_1^b$	$100w_2^b$	(k)	slope
$[C_2mim]BF_4 + (NH_4)_2C_4H_4O_6 + H_2O$								
288.15	37.85	9.64	48.09	5.96	27.82	13.30	−2.76	−2.76
	37.87	10.04	53.20	4.56	24.00	15.09	−2.77	
	37.58	10.57	56.53	3.74	20.88	16.70	−2.75	
	37.47	10.99	59.21	3.14	18.81	17.86	−2.74	
298.15	37.97	12.49	62.47	2.82	15.89	21.36	−2.51	−2.56
	39.93	10.06	54.67	4.54	22.75	16.62	−2.64	
	40.02	11.01	59.84	3.36	18.21	19.58	−2.57	
	40.07	12.01	64.12	2.50	14.96	22.13	−2.50	
308.15	40.12	12.53	65.09	2.63	16.57	22.05	−2.50	−2.52
	41.06	10.54	55.94	4.74	22.63	17.86	−2.54	
	41.10	10.99	58.83	4.02	20.41	19.27	−2.52	
	41.21	11.50	62.26	3.23	18.53	20.57	−2.52	
$[C_3mim]BF_4 + (NH_4)_2C_4H_4O_6 + H_2O$								
288.15	50.00	6.50	76.16	1.98	23.67	11.13	−5.74	−5.77
	50.04	6.10	72.19	2.15	25.89	10.13	−5.80	
	50.04	6.26	74.42	2.07	25.02	10.50	−5.86	
	50.17	6.82	78.94	1.80	22.52	11.72	−5.69	
298.15	44.85	8.22	63.18	4.19	25.73	12.49	−4.51	−4.44
	44.86	8.49	65.16	3.94	24.33	13.17	−4.42	
	44.98	8.99	68.52	3.48	21.70	14.54	−4.23	
	45.17	8.00	61.81	4.41	27.17	11.96	−4.59	
308.15	39.91	10.98	53.18	6.53	18.20	18.40	−2.95	−2.93
	39.95	11.99	58.93	5.55	16.17	20.21	−2.92	
	40.00	11.49	56.10	6.02	16.92	19.49	−2.91	
	40.09	10.63	51.21	6.89	18.87	17.89	−2.94	
$[C_4mim]BF_4 + (NH_4)_2C_4H_4O_6 + H_2O$								
288.15	44.91	3.51	75.61	0.39	17.13	6.37	−9.78	−9.77
	45.04	3.01	70.06	0.49	18.34	5.75	−9.83	
	45.06	3.70	78.19	0.35	17.74	6.60	−9.67	
	45.07	3.27	72.14	0.45	17.82	6.00	−9.79	
298.15	46.98	4.70	85.84	0.29	17.94	8.07	−8.73	−8.80
	47.05	4.50	84.05	0.30	18.23	7.82	−8.75	
	47.23	4.25	81.84	0.35	18.96	7.47	−8.83	
	47.63	3.91	78.67	0.43	19.96	7.03	−8.90	
308.15	47.96	4.84	86.49	0.18	21.44	8.11	−8.20	−8.38
	48.01	4.53	83.54	0.30	22.93	7.56	−8.35	
	48.02	4.28	80.67	0.43	24.33	7.10	−8.45	
	48.10	4.02	77.64	0.58	25.84	6.65	−8.53	

[a] Standard uncertainties u are $u(w)$ = 0.001, $u(T)$ = 0.05 K, and $u(p)$ = 10 kPa.

Table 9. Values of Parameters of eqs 10 and 11 for the $[C_2mim]BF_4/[C_3mim]BF_4/[C_4mim]BF_4$ (1) + $(NH_4)_2C_4H_4O_6$(2) + H_2O (3) ATPSs at T = (288.15, 298.15, and 308.15) K

T/K	$10^{-3}k_1$	n	k_2	r	R_1^2	R_2^2	$100sd_1$[a]	$100sd_2$[a]
			$[C_2mim]BF_4 + (NH_4)_2C_4H_4O_6 + H_2O$					
288.15	98.94640	1.27178	4.55240	0.55034	0.99706	0.99664	0.21	0.22
298.15	144.52400	1.08483	4.47899	0.70562	0.99565	0.99640	0.25	0.17
308.15	82.02950	1.48656	3.97045	0.50468	0.99448	0.99491	0.22	0.20
			$[C_3mim]BF_4 + (NH_4)_2C_4H_4O_6 + H_2O$					
288.15	3.61618	2.13533	8.86278	0.32542	0.97455	0.97506	0.35	0.29
298.15	43.81980	1.32698	6.93905	0.51184	0.99916	0.99938	0.07	0.05
308.15	44.91590	2.00341	3.82560	0.39044	0.98895	0.98980	0.24	0.26
			$[C_4mim]BF_4 + (NH_4)_2C_4H_4O_6 + H_2O$					
288.15	0.13721	2.88138	17.48357	0.32715	0.98507	0.99755	0.25	0.13
298.15	0.05644	3.28589	14.48939	0.25235	0.99458	0.99732	0.15	0.09
308.15	0.15181	2.86041	14.09841	0.25957	0.99819	0.99918	0.11	0.07

[a] $sd = [\sum_{i=1}^{N}((w_{i,j,cal}^{top} - w_{i,j,exp}^{top})^2 + (w_{i,j,cal}^{bot} - w_{i,j,exp}^{bot})^2)/2N]^{0.5}$, where N is the number of tie lines and j = 1 and j = 2; sd_1 and sd_2 represent the mass percent standard deviations for IL and salt, respectively.

the concentration of the two components is expressed in molality.

For a same salt in different component solvents, the phase-separation abilities of ILs increase with increasing EEV. As shown in Figure 2 and Table 7, it was found that the phase-separation abilities of the investigated ILs are in the order $[C_4mim]BF_4 > [C_3mim]BF_4 > [C_2mim]BF_4$. The increase in EEV is reflected by a decrease in the concentration of IL required for the formation of ATPS. The observation of Figure 2 indicates that the larger cation alkyl chain is, the greater is the IL's ability for ATPS formation. It is well-known that an increase in cation alkyl chain length leads to an increase of the IL's hydrophobic nature and therefore to a poorer affinity for water.[43] The higher the affinity for water and/or hydrophilic nature of the IL, the less effective is the IL in promoting ATPS. In general, ILs with lower water affinity require less salt to promote separation of two phases, resulting in a binodal curve closer to the axis and in a larger biphasic region.

Liquid–Liquid Equilibrium Data and Correlation. Recently, the lever rule has been successfully calculated the LLE data of IL–salt ATPSs.[15,16,18,44] In our previous research, we have demonstrated that the LLE data obtained by calculation via binodal curve and mass balance approach are reliable and valid.[45] In this paper, on the basis of eq 3 and the lever rule, the equilibrium compositions were calculated by MATLAB, using eqs 6–9 as follows

$$w_1^t = \exp[a + b(w_2^t)^{0.5} + cw_2^t + d(w_2^t)^2] \quad (6)$$

$$w_1^b = \exp[a + b(w_2^b)^{0.5} + cw_2^b + d(w_2^b)^2] \quad (7)$$

$$\frac{w_1^t - w_1}{w_1 - w_1^b} = \frac{m_b}{m_t} \quad (8)$$

$$\frac{w_2 - w_2^t}{w_2^b - w_2} = \frac{m_b}{m_t} \quad (9)$$

where w_1^t, w_1^b, w_2^t, and w_2^b represent the equilibrium compositions (in mass fraction) of IL (1) and salt (2), in the top, t, and bottom, b, phases, respectively. w_1 and w_2 represent the total compositions (in mass fraction) of IL (1) and salt (2)3 and 4, respectively. The results are given in Table 8 and Figures 3 and 4.

Table 10. Values of Parameters of eq 12 for the $[C_2mim]BF_4/[C_3mim]BF_4/[C_4mim]BF_4$ (1) + $(NH_4)_2C_4H_4O_6$(2) + H_2O (3) ATPSs at T = (288.15, 298.15, and 308.15) K

T/K	k	β	R^2	100 sd[a]
		$[C_2mim]BF_4 + (NH_4)_2C_4H_4O_6 + H_2O$		
288.15	4.62845	0.14386	0.99865	0.25
298.15	5.07634	0.33202	0.99735	0.33
308.15	5.26520	0.44060	0.99724	0.30
		$[C_3mim]BF_4 + (NH_4)_2C_4H_4O_6 + H_2O$		
288.15	3.22452	−0.04406	0.98607	0.33
298.15	3.55238	0.23700	0.99890	0.12
308.15	3.25618	0.10072	0.99979	0.05
		$[C_4mim]BF_4 + (NH_4)_2C_4H_4O_6 + H_2O$		
288.15	5.31410	0.29305	0.99065	0.25
298.15	5.9674	0.69845	0.9834	0.35
308.15	10.28262	2.94066	0.98122	0.59

[a] $sd = [\sum_{j=1}^{3}\sum_{i=1}^{N}((w_{i,j,cal}^{top} - w_{i,j,exp}^{top})^2 + (w_{i,j,cal}^{bot} - w_{i,j,exp}^{bot})^2)/6N]^{0.5}$, where N is the number of tie-lines and j is the number of components in each phase.

The reliability of the tie-line compositions is ascertained by the empirical correlation equations given by Othmer–Tobias (eq 10) and Bancroft (eq 11).

$$\left(\frac{1 - w_1^t}{w_1^t}\right) = k_1\left(\frac{1 - w_2^b}{w_2^b}\right)^n \quad (10)$$

$$\left(\frac{w_3^b}{w_2^b}\right) = k_2\left(\frac{w_3^t}{w_1^t}\right)^r \quad (11)$$

where w_1^t is the mass fraction of ILs in the top phase, w_2^b is the mass fraction of salt in the bottom phase, w_3^b and w_3^t are the mass fraction of water in the bottom and top phases, respectively, and k_1, n, k_2, and r are the fit parameters. A linear dependency of the plots

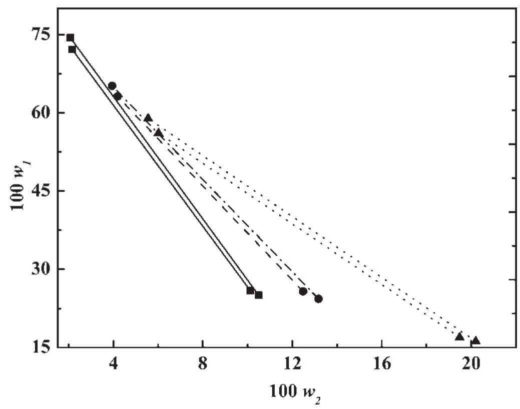

Figure 3. Effect of temperature on the equilibrium phase compositions of the $[C_3mim]BF_4$ (1) + $(NH_4)_2C_4H_4O_6$ (2) + H_2O (3) ATPS: ■, 288.15 K; ●, 298.15 K; ▲, 308.15 K; —, tie lines at 288.15 K; ---, tie lines at 298.15 K; · · ·, tie lines at 308.15 K. These tie lines were obtained by connecting the experimental equilibrium phase composition data.

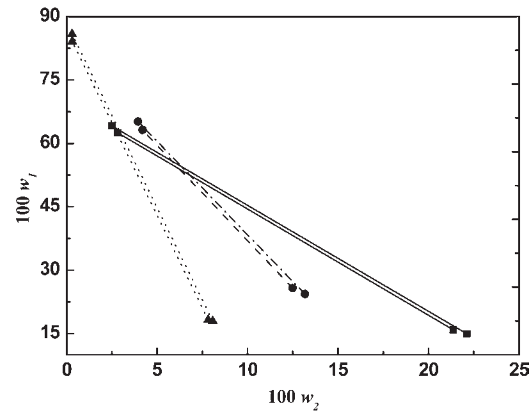

Figure 4. Effect of type of IL on the equilibrium phase compositions of the $[C_2mim]BF_4$/$[C_3mim]BF_4$/$[C_4mim]BF_4$ (1) + $(NH_4)_2C_4H_4O_6$ (2) + H_2O (3) ATPS at 298.15 K: ■, $[C_2mim]BF_4$; ●, $[C_3mim]BF_4$; ▲, $[C_4mim]BF_4$; —, tie lines at $[C_2mim]BF_4$; ---, tie lines at $[C_3mim]BF_4$; · · ·, tie lines at $[C_4mim]BF_4$. These tie lines were obtained by connecting the experimental equilibrium phase composition data.

$\log[(1-w_1^t)/w_1^t]$ against $\log[(1-w_2^b)/w_2^b]$ and $\log(w_3^b/w_2^b)$ against $\log(w_3^t/w_1^t)$ indicated an acceptable consistency of the results. The values of the parameters k_1, n, k_2, and r of equations with the corresponding correlation coefficient values (R^2) and standard deviations (sd) are given in Table 9, and the results show a good reliability of the calculation method and the corresponding tie-line data.

In this work, a relatively simple two-parameter equation was used to correlate the tie-line data, which can be derived from the binodal theory.[39] The equation used has the following form:

$$\ln\left(\frac{w_2^t}{w_2^b}\right) = \beta + k(w_1^b - w_1^t) \tag{12}$$

In which the k is the salting-out coefficient and β is the constant related to the activity coefficient. Superscripts "t" and "b" stand for the IL-rich phase and salt-rich phase, respectively. The fitting parameters of eq 12, along with the corresponding standard deviations, are presented in Table 10 for the investigated systems. On the basis of the standard deviations reported in Table 10, eq 12 represents the experimental LLE data with a good accuracy at each temperature.

Effect of Temperature on TLs. Table 8 shows the values of tie-line slope of $[C_2mim]BF_4$/$[C_3mim]BF_4$/$[C_4mim]BF_4$−$(NH_4)_2C_4H_4O_6$ ATPSs at different temperatures. Additionally, to show the effect of temperature on the equilibrium phase compositions for the investigated system, the experimental tie lines of $[C_3mim]BF_4$−$(NH_4)_2C_4H_4O_6$ ATPSs are compared in Figure 3 for the temperatures T = (288.15, 298.15, and 308.15) K. As shown in Figure 3, it was found that the absolute value of slope of the tie lines slightly decrease with an increase in temperature. This trend means that when the temperature is decreased, water is driven from the $[C_3mim]BF_4$-rich phase to the salt-rich phase, so the $[C_3mim]BF_4$ concentration at the $[C_3mim]BF_4$-rich phase increases, whereas the salt-rich phase will be somewhat more diluted. In other words, water becames a poorer solvent for $[C_3mim]BF_4$ as the temperature is decreased. This is because the compositions of the phases in equilibrium change with varying temperature.

Effect of the Type of IL on TLs. To show the effect of IL cation alkyl chain length on the phase compositions, the tie lines for the $[C_2mim]BF_4$/$[C_3mim]BF_4$/$[C_4mim]BF_4$−$(NH_4)_2C_4H_4O_6$ ATPSs at T = 298.15 K are compared and depicted in Figure 4. As can be seen, the slope of tie line increases with an increase in cation alkyl chain length. The possible reason is that an increased IL cation alkyl chain length for IL−salt ATPSs causes the water to drive preferably from the IL-rich phase to the salt-rich phase, so the IL concentration at the IL-rich phase increases, while the required salt will be decreased. This is the same as the phase-separartion abilities of the investigated ILs.

■ CONCLUSIONS

Binodal data of the $[C_2mim]BF_4$/$[C_3mim]BF_4$/$[C_4mim]BF_4$−$(NH_4)_2C_4H_4O_6$ ATPSs were determined and correlated at T = (288.15, 298.15, and 308.15) K. On the basis of the highest accuracy fitting equation of binodal data and lever rule, the liquid−liquid equilibrium data were directly calculated by MATLAB. The reliability of the calculation method and the corresponding LLE data was proved by the Othmer−Tobias and the Bancroft equations. Moreover, the tie-line data were successfully correlated with a relatively simply two-parameter equation. Using the binodal model, the EEV was calculated for these three systems at different temperatures. For a same salt in different component solvents, the phase-separation abilities of ILs increase with increasing EEV. It was found that the phase-separation abilities of the investigated ILs are in the order $[C_4mim]BF_4$ > $[C_3mim]BF_4$ > $[C_2mim]BF_4$. The two-phase area was expanded with a decrease in temperature, while the slope of the tie lines was decreased with an increase in temperature.

■ AUTHOR INFORMATION

Corresponding Author

*E-mail: yys@ujs.edu.cn. Tel: 86-0511-88790683. Fax: +86-0511-88791800.

Funding Sources

This work has been supported by the National Natural Science Foundation of China (No. 21076098), the Natural Science Foundation of Jiangsu Province (No. BK2010349), the Ph.D. Programs Foundation of Ministry of Education of China (No. 200807100004), Programs of Senior Talent Foundation of Jiangsu University (11JDG029), and a China Postdoctoral Science Foundation Funded Project (No. 1611310015).

■ REFERENCES

(1) Albertsson, P. A. *Partitioning of Cell Particles and Macromolecules*; J. Wiley & Sons: New York, 1986.

(2) Walter, H.; Brooks, D. E.; Fisher, D. *Partitioning in Aqueous Two-Phase systems*; Academic Press: New York, 1985.

(3) Zaslavsky, B. Y. *Aqueous Two-Phase Partitioning, Physical Chemistry and Bioanalytical Applications*; Marcel Dekker: New York, 1995.

(4) Han, X.; Armstrong, D. W. Ionic liquids in separations. *Acc. Chem. Res.* **2007**, *40*, 1079–1086.

(5) Gutowski, K. E.; Broker, G. A.; Willauer, H. D.; Huddleston, J. G.; Swatloski, R. P.; Holbrey, J. D.; Rogers, R. D. Controlling the aqueous miscibility of ionic Liquids: aqueous biphasic systems of water-miscible ionic liquids and water-structuring salts for recycle, metathesis, and separations. *J. Am. Chem. Soc.* **2003**, *125*, 6632–6633.

(6) He, C.; Li, S.; Liu, H.; Li, K.; Liu, F. Extraction of testosterone and epitestosterone in human urine using aqueous two-phase systems of ionic liquid and salt. *J. Chromatogr. A* **2005**, *1082*, 143–149.

(7) Li, S.; He, C.; Liu, H.; Li, K.; Liu, F. Ionic liquid-based aqueous two-phase system, a sample pretreatment procedure prior to high-performance liquid chromatography of opium alkaloids. *J. Chromatogr. B* **2005**, *826*, 58–62.

(8) Du, Z.; Yu, Y. L.; Wang, J. H. Extraction of proteins from biological fluids by use of an ionic liquid/aqueous two-phase system. *Chem.—Eur. J.* **2007**, *13*, 2130–2137.

(9) Pei, Y.; Wang, J.; Wu, K.; Xuan, X.; Lu, X. Ionic liquid-based aqueous two-phase extraction of selected proteins. *Sep. Purif. Technol.* **2009**, *64*, 288–295.

(10) Neves, C. M. S. S.; Ventura, S. P. M.; Freire, M. G.; Marrucho, I. M.; Coutinho, J. A. P. Evaluation of cation influence on the formation and extraction capability of ionic-liquid-based aqueous biphasic systems. *J. Phys. Chem. B* **2009**, *113*, 5194–5199.

(11) Ventura, S. P. M.; Neves, C. M. S. S.; Freire, M. G.; Marrucho, I. M.; Oliveira, J.; Coutinho, J. A. P. Evaluation of anion influence on the formation and extraction capacity of ionic-liquid-based aqueous biphasic systems. *J. Phys. Chem. B* **2009**, *113*, 9304–9310.

(12) Li, C. X.; Han, J.; Wang, Y.; Yan, Y. S.; Xu, X. H.; Pan, J. M. Extraction and mechanism investigation of trace roxithromycin in real water samples by use of ionic liquid-salt aqueous two-phase system. *Anal. Chim. Acta* **2009**, *653*, 178–183.

(13) Han, J.; Wang, Y.; Yu, C. L.; Yan, Y. S.; Xie, X. Q. Extraction and determination of chloramphenicol in feed water, milk, and honey samples using an ionic liquid/sodium citrate aqueous two-phase system coupled with high-performance liquid chromatography. *Anal Bioanal. Chem.* **2011**, *399*, 1295–1304.

(14) Li, Z.; Pei, Y.; Liu, L.; Wang, J. (Liquid + liquid) equilibria for (acetate-based ionic liquids + inorganic salts) aqueous two-phase systems. *J. Chem. Thermodynamics* **2010**, *42*, 932–937.

(15) Deive, F. J.; Rivas, M. A.; Rodríguez, A. Sodium carbonate as phase promoter in aqueous solutions of imidazolium and pyridinium ionic liquids. *J. Chem. Thermodynamics* **2011**, *43*, 1153–1158.

(16) Deng, Y.; Long, T.; Zhang, D.; Chen, J.; Gan, S. Phase diagram of [Amim]Cl + salt aqueous biphasic systems and its application for [Amim]Cl recovery. *J. Chem. Eng. Data* **2009**, *54*, 2470–2473.

(17) Bridges, N. J.; Gutowski, K. E.; Rogers, R. D. Investigation of aqueous biphasic systems formed from solutions of chaotropic salts with kosmotropic salts (salt—salt ABS). *Green Chem.* **2007**, *9*, 177–183.

(18) Deng, Y.; Chen, J.; Zhang, D. Phase diagram data for several salt + salt aqueous biphasic systems at 298.15 K. *J. Chem. Eng. Data* **2007**, *52*, 1332–1335.

(19) Zafarani-Moattar, M. T.; Hamzehzadeh, S. Liquid—liquid equilibria of aqueous two-phase systems containing 1-butyl-3-methylimidazolium bromide and potassium phosphate or dipotassium hydrogen phosphate at 298.15 K. *J. Chem. Eng. Data* **2007**, *52*, 1686–1692.

(20) Li, C. X.; Han, J.; Wang, Y.; Yan, Y. S.; Pan, J. M.; Xu, X. H.; Zhang., Z. L. Phase behavior for the aqueous two-phase systems containing the ionic liquid 1-buty-3-methylimidazolium tetrafluoroborate and kosmotropic salts. *J. Chem. Eng. Data* **2010**, *55*, 1087–1092.

(21) Zhang, Y.; Zhang, S.; Chen, Y.; Zhang, J. Aqueous biphasic systems composed of ionic liquid and fructose. *Fluid Phase Equilib.* **2007**, *257*, 173–176.

(22) Wu, B.; Zhang, Y.; Wang, H. Phase behavior for ternary systems composed of ionic liquid + saccharides + water. *J. Phys. Chem. B* **2008**, *112*, 6426–6429.

(23) Wu, B.; Zhang, Y.; Wang, H.; Yang, L. Temperature dependence of phase behavior for ternary systems composed of ionic liquid + sucrose + water. *J. Phys. Chem. B* **2008**, *112*, 13163–13165.

(24) Wu, B.; Zhang, Y. M.; Wang, H. P. Aqueous biphasic systems of hydrophilic ionic liquids + sucrose for separation. *J. Chem. Eng. Data* **2008**, *53*, 983–985.

(25) Chen, Y.; Meng, Y.; Zhang, S.; Zhang, Y.; Liu, X.; Yang, J. Liquid—liquid equilibria of aqueous biphasic systems composed of 1-butyl-3-methyl imidazolium tetrafluoroborate + sucrose/maltose + water. *J. Chem. Eng. Data* **2010**, *55*, 3612–3616.

(26) Chen, Y.; Zhang, S. Phase behavior of (1-alkyl-3-methyl imidazolium tetrafluoroborate + 6-(hydroxymethyl)oxane-2,3,4,5-tetrol + water). *J. Chem. Eng. Data* **2010**, *55*, 278–282.

(27) Zhang, J.; Zhang, Y.; Chen, Y.; Zhang, S. Mutual coexistence curve measurement of aqueous biphasic systems composed of [bmim][BF_4] and glycine, l-serine, and l-proline, respectively. *J. Chem. Eng. Data* **2007**, *52*, 2488–2490.

(28) Zafarani-Moattar, M. T.; Hamzehzadeh, S. Salting-out effect, preferential exclusion, and phase separation in aqueous solutions of chaotropic water-miscible ionic liquids and kosmotropic salts: effects of temperature, anions, and cations. *J. Chem. Eng. Data* **2010**, *55*, 1598–1610.

(29) Zafarani-Moattar, M. T.; Hamzehzadeh, S. Phase diagrams for the aqueous two-phase ternary system containing the ionic liquid 1-butyl-3-methylimidazolium bromide and tri-potassium citrate at T = (278.15, 298.15, and 318.15) K. *J. Chem. Eng. Data* **2009**, *54*, 833–841.

(30) Zafarani-Moattar, M. T; Hamzehzadeh, S. Effect of pH on the phase separation in the ternary aqueous system containing the hydrophilic ionic liquid 1-butyl-3-methylimidazolium bromide and the kosmotropic salt potassium citrate at T = 298.15 K. *Fluid Phase Equilib.* **2011**, *304*, 110–120.

(31) Han, J.; Yu, C. L.; Wang, Y.; Xie, X. Q.; Yan, Y. S.; Yin, G. W.; Guan, W. X. Liquid—liquid equilibria of ionic liquid 1-butyl-3-methylimidazolium tetrafluoroborate and sodium citrate/tartrate/acetate aqueous two-phase systems at 298.15 K: Experiment and correlation. *Fluid Phase Equilib.* **2010**, *295*, 98–103.

(32) Han, J.; Pan, R.; Xie, X. Q.; Wang, Y.; Yan, Y. S.; Yin, G. W.; Guan, W. X. Liquid-liquid Equilibria of ionic liquid 1-butyl-3-methylimidazolium tetrafluoroborate + sodium and ammonium citrate aqueous two-phase systems at (298.15, 308.15 and 323.15) K. *J. Chem. Eng. Data* **2010**, *55*, 3749–3754.

(33) Merchuk, J. C.; Andrews, B. A.; Asenjo, J. A. Aqueous two-phase systems for protein separation: Studies on phase inversion. *J. Chromatogr. B* **1998**, *711*, 285–293.

(34) Pei, Y.; Wang, J.; Liu, L.; Wu, K.; Zhao, Y. Liquid—liquid equilibria of aqueous biphasic systems containing selected imidazolium ionic liquids and salts. *J. Chem. Eng. Data* **2007**, *52*, 2026–2031.

(35) Ferreira, L. A.; Teixeira, J. A. Salt effect on the aqueous two-phase system PEG 8000-sodium sulfate. *J. Chem. Eng. Data* **2011**, *56*, 133–137.

(36) Foroutan, M. Liquid—liquid equilibria of aqueous two-phase poly(vinylpyrrolidone) and K_2HPO_4/KH_2PO_4 buffer: effects of pH and temperature [J]. *J. Chem. Eng. Data* **2007**, *52*, 859–862.

(37) Shekaari, H.; Sadeghi, R.; Jafari, S. A. Liquid—liquid equilibria for aliphatic alcohols + dipotassium oxalate + water. *J. Chem. Eng. Data* **2010**, *55*, 4586–4591.

(38) Wang, Y.; Hu, S. P.; Han, J.; Yan, Y. S. Measurement and correlation of phase diagram data for several hydrophilic alcohol + citrate

aqueous two-phase systems at 298.15 K. *J. Chem. Eng. Data* **2010**, *55*, 4574–4579.

(39) Guan, Y.; Lilley, T. H.; Treffry, T. E. A new excluded volume theory and its application to the coexistence curves of aqueous polymer two-phase systems. *Macromolecules* **1993**, *26*, 3971–3979.

(40) Wang, Y.; Hu, S. P.; Yan, Y. S.; Guan, W. S. Liquid-liquid equilibrium of potassium/sodium carbonate + 2-propanol/ethanol + water aqueous two-phase systems and correlation at 298.15 K. *Calphad* **2009**, *33*, 726–731.

(41) Xie, X. Q.; Yan, Y. S.; Han, J.; Wang, Y.; Yin, G. W.; Guan, W. S. Liquid-liquid equilibrium of aqueous two-phase systems of PPG400 and biodegradable salts at temperatures of (298.15, 308.15, and 318.15) K. *J. Chem. Eng. Data* **2010**, *55*, 2857–2861.

(42) Xie, X. Q.; Han, J.; Wang, Y.; Yan, Y. S.; Yin, G. W.; Guan, W. S. Measurement and correlation of the phase diagram data for PPG400 + (K_3PO_4, K_2CO_3, and K_2HPO_4) + H_2O aqueous two-phase systems at T = 298.15 K. *J. Chem. Eng. Data* **2010**, *55*, 4741–4745.

(43) Freire, M. G.; Neves, C. M. S. S.; Carvalho, P. J.; Gardas, R. L.; Fernandes, A. M.; Marrucho, I. M.; Santos, L. M. N. B. F.; Coutinho, J. A. P. Mutual solubilities of water and hydrophobic ionic liquids. *J. Phys. Chem. B* **2007**, *111*, 13082–13089.

(44) Neves, C. M. S. S.; Ventura, S. P. M.; Freire, M. G.; Marrucho, I. M.; Coutinho, J. A. P. Evaluation of cation influence on the formation and extraction capability of ionic-liquid-based aqueous biphasic systems. *J. Phys. Chem. B* **2009**, *113*, 5194–5199.

(45) Wang, Y.; Yan, Y. S.; Hu, S. P.; Han, J.; Xu, X. H. Phase diagrams of ammonium sulfate + ethanol/1-propanol/2-propanol + water aqueous two-phase systems at 298.15 K and correlation. *J. Chem. Eng. Data* **2010**, *55*, 876–881.